Influence of annealing temperature on microstructure and H_2 sensing properties of Pd-doped SnO_2 sputtered thin films

Yanbai SHEN[1,a*], Anfeng FAN[1,b], Dezhou WEI[1,c], Shuling GAO[1,d], Baoyu CUI[1,e] and Lijun JIA[1,f]

[1]College of Resources and Civil Engineering, Northeastern University, Shenyang 110819, China

[2]JangHo Architecture College of NEU, Northeastern University, Shenyang 110819, China

[a]shenyanbai@mail.neu.edu.cn, [b]afnshqq@163.com, [c]dzwei@mail.neu.edu.cn, [d]gaoshuling@mail.neu.edu.cn, [e]cuibaoyu@mail.neu.edu.cn, [f]jialijun@mail.neu.edu.cn

Keywords: SnO_2 Thin Film; Palladium; Annealing; Hydrogen; Gas Sensor

Abstract. The influence of annealing temperature on the microstructure and H_2 sensing properties of Pd-doped SnO_2 sputtered thin films were investigated. The as-deposited film was amorphous and would crystallize to tetragonal SnO_2 structure when the annealing temperature was above 350°C. The films were composed of columnar grains. Both crystallite size and grain size increased with an increase in annealing temperature. H_2 sensing measurements showed that gas sensors based on these films obtained the peak response to 1000 ppm H_2 at an operating temperature of 100°C and showed a good reversibility. The Pd-doped SnO_2 thin film annealed at 450°C showed the highest response to H_2. The improved gas sensing properties were attributed to the porosity of columnar nanostructures and catalytic activities of Pd doping.

1. Introduction

In recent years, oxide semiconductor gas sensors have attracted significant attention due to their simple implementation, low cost, and good reliability for real-time control system with respect to other gas sensor devices [1]. Different materials such as SnO_2, WO_3, ZnO have been investigated and show promising applications for detecting target gases such as H_2, H_2S, NO_2, etc [2–4]. Although some gas sensors based on oxide semiconductors have been commercialized for years, many problems still need to be solved to improve the sensitivity, stability, selectivity, and reliability.

The gas sensing properties of oxide semiconductors are usually influenced by many microstructure factors such as grain size, film thickness, porosity, dopants, and so on. The response of an oxide semiconductor gas sensor comes from the change in the electrical conductivity or resistance due to the change in the gas atmosphere surrounding the sensor. The detected gas molecules react with surface adsorbed species (O_2^-, O^- and O^{2-}, etc.) of oxide semiconductor gas sensor [5]. Therefore, the control of microstructure and the fundamental mechanism of microstructure effects are two of the main themes of the research on oxide semiconductor gas sensor.

As an n-type wide band gap semiconductor material (E_g=3.6 eV at 300 K), SnO_2 is a key functional material that has been used extensively for transparent conductors [6], gas sensors [7], transistors [8], and optoelectronic devices [9]. Preparation techniques such as magnetron sputtering, chemical vapour deposition, thermal evaporation, sol-gel process, and pulsed laser deposition have been used to deposit SnO_2 thin films. Most of these methods require a post-annealing process to stabilize the film structure and improve the operating performance of gas sensors. However, annealing leads to the change not only of crystallinity but also of the grain size and density of adsorption sites. Therefore, it is necessary to understand the effect of annealing on the microstructure and gas sensing properties of oxide semiconductors. In this study, SnO_2 thin films were prepared by sputtering method and annealed at different temperatures. The films were doped with Pd to further improve gas sensing properties. The effect of annealing temperature on the microstructure and H_2 sensing properties of the Pd-doped SnO_2 thin films were systematically investigated.

2. Experimental

Pd-doped SnO_2 thin films with a thickness of approximately 300 nm were deposited on oxidized Si substrates at room temperature (RT) by dc reactive magnetron sputtering. A circular tin target of 100 mm in diameter with a purity of 99.99% was used. For Pd doping, two pieces of Pd chips with a thickness of 0.1 mm were pasted on the tin target using silver paste at the most deeply eroded points which were 26 mm away from the tin target center. The target was then baked at 200°C for 2 h in drying oven before sputtering. Pd concentration in the films was evaluated to be about 4 at.% using an energy-dispersive X-ray analyzer. The discharge gas was an argon–oxygen mixture with a ratio of $Ar:O_2=2:3$. The chamber was first evacuated to 4×10^{-4} Pa and then was kept at 12 Pa during the film deposition by filling the discharge gas. The discharge current was fixed at 80 mA, and the discharge voltage showed a value of about 300 V. Before the deposition, the target was pre-sputtered for 5 min with a shutter closed. After the deposition, the films were annealed at different temperatures between 350 and 650°C for 4 h in air with a heating and cooling rate of 2°C min^{-1} to stabilize the film structure. When the film was used as a sensor, a pair of Pt interdigital electrodes with a gap length of 0.12 mm was formed on Si substrates before the film deposition.

The crystallographic structure of the films was investigated by X-ray diffraction (XRD) using an X-ray diffractometer (PANalytical X'Pert Pro) with Cu Kα radiation. The incident angle was 0.5°. The morphology of the films was observed by using a field emission scanning electron microscope (FESEM, ZEISS Ultra Plus) with the operating voltage of 20 kV.

H_2 sensing measurements were carried out in an aluminum chamber with a capacity of 13×10^{-3} m^3 in ambient air. The sensors were heated from the back of the substrate using an electric heater. The heater was made of a nichrome wire wound around a mica plate and was sandwiched between two mica plates. A chromel-alumel thermocouple was fixed beside the gas sensors for the thermometry, and the operating temperature was changed from 50 to 300°C. H_2 was introduced into the chamber to a predefined concentration of 1000 ppm using an injector and stirred by circulating the ambient air using a pump installed outside the chamber. The resistance of the sensors was determined by measuring the electric current which flowed when a voltage of 10 V was applied between Pt interdigital electrodes. For this measurement, a computerized Agilent 34972A multimeter was used. The response of the sensor was defined as $(R_a-R_g)/R_g$, where R_a and R_g were the electrical resistances before and after the introduction of H_2, respectively.

3. Results and discussion

Fig. 1 shows the XRD patterns of the as-deposited film and the films annealed at the temperatures of 350, 450, 550, and 650°C. The structure of the as-deposited film was amorphous while a tetragonal structure was formed in the films annealed at 350°C or above. For the annealed films, all the diffraction peaks could be indexed to the tetragonal SnO_2 structure with lattice constants of a=b=0.4738 nm and c=0.3187 nm according to JCPDS card No. 41-1445. The diffraction peaks became sharp with increasing annealing temperatures from 350 to 650°C, indicating the improvement of crystallinity. In addition, no peaks related to Pd were observed from the XRD patterns due to low Pd concentration in the films.

The surface and cross-sectional FESEM images of the as-deposited film and the films annealed at different temperatures are shown in Fig. 2. As shown in this figure, all the films deposited at a relatively high discharge gas pressure of 12 Pa were generally composed of columnar grains. The grain size, namely, the thickness of columnar grain, increased with increasing the annealing temperature as shown later in Fig. 3. Sintering of the grains was promoted and the film was densified as the annealing temperature increased, resulting in an increase in the grain size and the formation of cracks. The increase in grain size with increasing annealing temperature observed here agrees with those reported by Satapathy et al. [10] and Wu et al. [11] for $LiTaO_3$ thin films and VO_2 films, respectively.

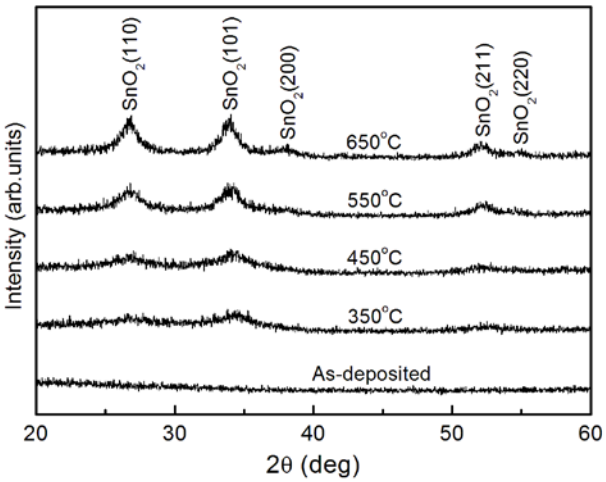

Fig. 1 XRD patterns of the Pd-doped SnO_2 thin films deposited at 12 Pa and RT. The results of the as-deposited film and the films annealed at 350, 450, 550, and 650°C are shown.

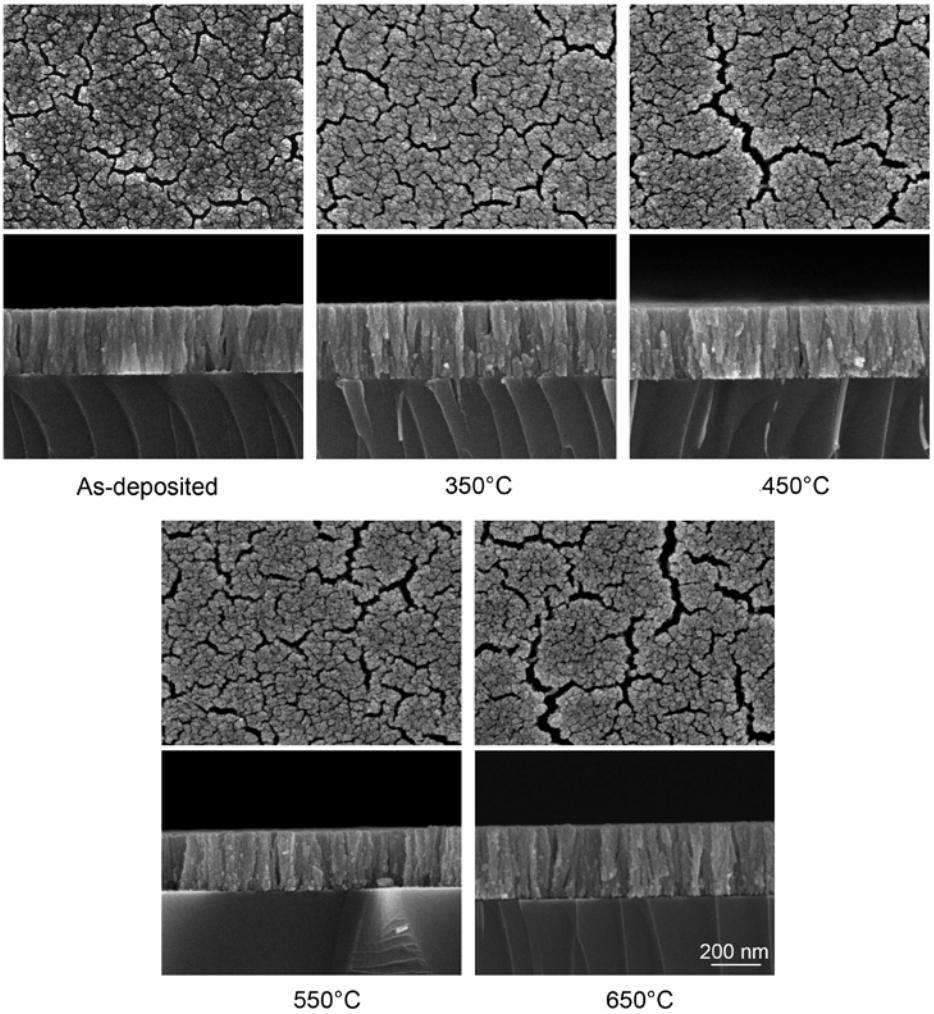

Fig. 2 Surface and cross-sectional FESEM images of the Pd-doped SnO_2 films deposited at 12 Pa and RT. The images of the as-deposited film and the films annealed at 350, 450, 550, and 650°C are shown.

The crystallite size calculated by Scherrer's formula from the XRD patterns and the grain size observed by FESEM images are represented in Fig. 3 as a function of the annealing temperature. As shown in this figure, the crystallite size increased from 2.4 to 6.2 nm as the annealing temperature increased from 350 to 650°C. On the other hand, the grain size observed from FESEM images varied from 24 to 32 nm as the annealing temperature increased from 350 to 650°C. Especially, it should be noted that the grain size was larger than the crystallite size for the same film, indicating that the grains were composed of some small crystallites.

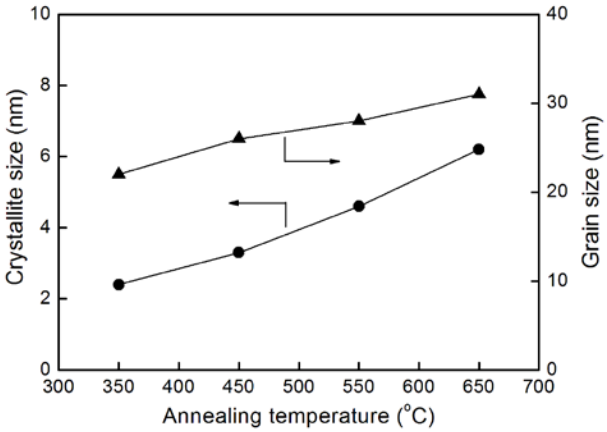

Fig. 3 Crystallite size and grain size of the films as a function of the annealing temperature.

Fig. 4 shows the typical examples of the changes in the resistance of the films annealed at different temperatures upon exposure to 1000 ppm H_2 at an operating temperature of 100°C. The resistance in air decreased from 23.4 to 6.9 MΩ as the annealing temperature increased from 350 to 650°C. Such decrease in the resistance results from more close contact between columnar grains at a higher annealing temperature. In addition, the resistance decreased rapidly upon exposure to H_2 and almost saturated within 300 s except for the film annealed at 350°C, and the resistance could recover to its initial value after H_2 removal, indicating a good reversibility. Especially, the maximal change in the resistance was found for the film annealed at 450°C, revealing that this film obtained the highest response to H_2.

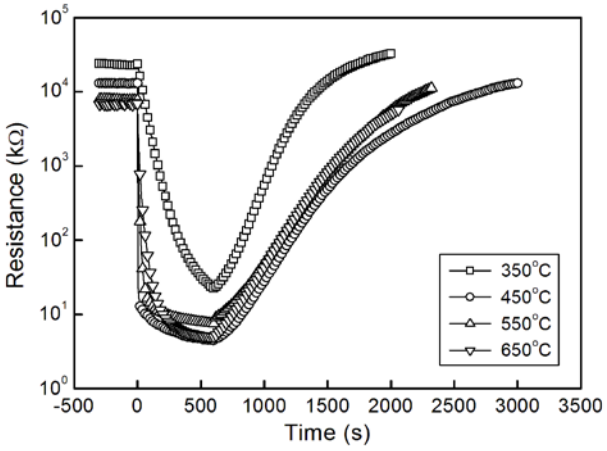

Fig. 4 Typical examples of the changes in the resistance of the films annealed at different temperatures upon exposure to 1000 ppm H_2 at an operating temperature of 100°C.

The relationship between the response to 1000 ppm H_2 and operating temperature for the films annealed at different temperatures is shown in Fig. 5. As shown in this figure, it should be noted that the responses of the film annealed at 350°C were of poor at the operating temperatures of 50 and 100°C because the resistance in H_2 did not saturate after exposure to H_2 for 600 s as the time for the definition of the response; this means the response would be higher if the exposure time is selected longer. The peak response was found at an operating temperature of 100°C for every film. The highest response was obtained for the film annealed at 450°C. As the annealing temperature increased, the columnar grains came to more close contact with each other. Therefore, the response gradually decreased.

According to the above-mentioned result, the relationship between the peak response to 1000 ppm H_2 and annealing temperature at an operating temperature of 100 °C is shown in Fig. 6. The response of the film annealed at 350°C was 1060, and the highest response of 2978 was obtained for the film annealed at 450°C. As the annealing temperature further increased, the responses of the films decreased to 1983 and 1421 at the annealing temperatures of 550 and 650°C, respectively. As shown in Fig. 2, the columnar grains using to compose of the film gradually came to more close contact with

each other as the annealing temperature increased, resulting in the highest response at the annealing temperature of 450°C.

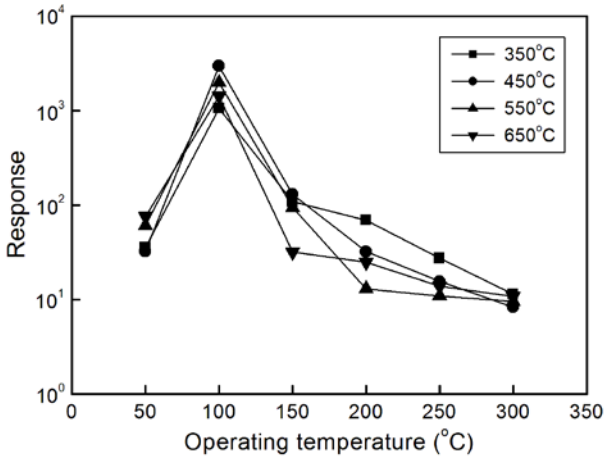

Fig. 5 Relationship between the response to 1000 ppm H_2 and operating temperature for the films annealed at different temperatures.

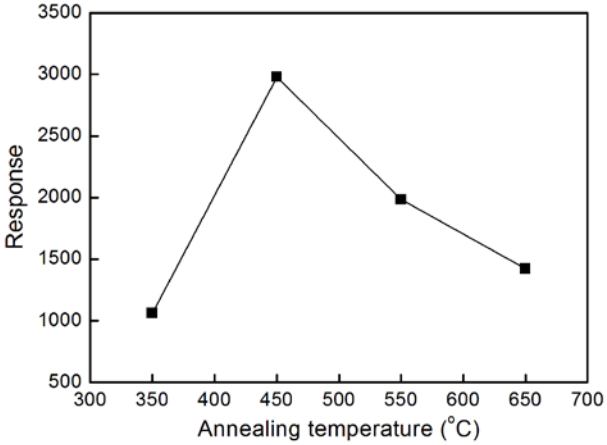

Fig. 6 Relationship between the peak response to 1000 ppm H_2 and annealing temperature at an operating temperature of 100°C.

At a high discharge gas pressure of 12 Pa, the contact area between neighboring grains decreases and the film becomes porous, which leads to the formation of the film with a large surface area. Thus, the response is greatly enhanced for these porous films. On the other hand, as the film porosity increases, the features of Schottky-barrier-limited transport prevail while the bulk transport features diminish [12], which results in the decrease of the operating temperature at which the response shows a maximum. Moreover, Pd doping further enhances the response and lowers the operating temperature by so-called chemical and electronic effects [13,14].

4. Conclusions

In this study, XRD, FESEM, and H_2 sensing measurements have been carried out to investigate the Pd-doped SnO_2 sputtered thin films annealed at different temperatures. The as-deposited film was amorphous and would crystallize to tetragonal SnO_2 structure when the annealing temperature was at 350°C or above. The crystallite size and grain size increased from 2.4 to 6.2 nm and from 24 to 32 nm, respectively, with increasing the annealing temperature from 350 to 650°C. All the film sensors showed the peak response to H_2 at an operating temperature of 100°C. The response and recovery times became short as the annealing temperature increased except for the film annealed at 350°C. The highest response of 2978 to 1000 ppm H_2 was obtained for the film annealed at 450°C. The results highlight the importance of achieving porous structure and noble metal doping on improving the gas sensing performance. By taking advantage of the annealing process, the microstructural parameters of sputtered films can be controlled to fit the request for gas sensor application.

Acknowledgement

The project was supported by the National Natural Science Foundation of China (51422402), Fundamental Research Funds for the Central Universities (N140105002), Program for Liaoning Excellent Talents in University (LJQ2013025), Specialized Research Fund for the Doctoral Program of Higher Education of China (20130042120033), and Scientific Research Foundation for the Returned Overseas Chinese Scholars, State Education Ministry (47-3).

References

[1] A. Vomiero, I. Concina, E. Comini, C. Soldano, M. Ferroni, G. Faglia, G. Sberveglieri, One-dimensional nanostructured oxides for thermoelectric applications and excitonic solar cells, Nano Energy 1 (2012) 372-390.

[2] Y. B. Shen, D. Z. Wei, M. Y. Li, W. G. Liu, S. L. Gao, C. Han, B. Y. Cui, Microstructure and room-temperature H_2 sensing properties of undoped and impurity-doped SnO_2 nanowires, Chem. Lett. 42 (2013) 492-494.

[3] C. M. Ghimbeu, M. Lumbreras, M. Siadat, J. Schoonman, Detection of H_2S, SO_2, and NO_2 using electrostatic sprayed tungsten oxide films, Mater. Sci. Semicond. Process. 13 (2010) 1-8.

[4] S. H. Wei, Y. Yu, M. H. Zhou, CO gas sensing of Pd-doped ZnO nanofibers synthesized by electrospinning method, Mater. Lett. 64 (2010) 2284-2286.

[5] B. Ruhland, T. Becker, G. Müller, Gas-kinetic interactions of nitrous oxides with SnO_2 surfaces, Sens. Actuators, B 50 (1998) 85-94.

[6] D. Vaufrey, M. B. Khalifa, M. P. Besland, C. Sandu, M. G. Blanchin, V. Teodorescu, J. A. Roger, J. Tardy, Reactive ion etching of sol-gel-processed SnO_2 transparent conducting oxide as a new material for organic light emitting diodes, Synth. Met. 127 (2002) 207-211.

[7] Y. Shimizu, A. Jono, T. Hyodo, M. Egashira, Preparation of large mesoporous SnO_2 powder for gas sensor application, Sens. Actuators, B 108 (2005) 56-61.

[8] J. C. Chou, Y. F. Wang, Preparation and study on the drift and hysteresis properties of the tin oxide gate ISFET by the sol-gel method, Sens. Actuators, B 86 (2002) 58-62.

[9] Z. Ying, Q. Wan, Z. T. Song, S. L. Feng, Controlled synthesis of branched SnO_2 nanowhiskers, Mater. Lett. 59 (2005) 1670-1672.

[10] S. Satapathy, K. B. R. Varma, Orientated nano grain growth and effect of annealing on grain size in $LiTaO_3$ thin films deposited by sol-gel technique, J. Cryst. Growth 291 (2006) 232-238.

[11] J. Wu, W. X. Huang, Q. W. Shi, J. H. Cai, D. Zhao, Y. B. Zhang, J. Z. Yan, Effect of annealing temperature on thermochromic properties of vanadium dioxide thin films deposited by organic sol-gel method, Appl. Surf. Sci. 268 (2013) 556-560.

[12] R. Botter, T. Aste, D. Beruto, Influence of microstructures on the functional properties of tin oxide-based gas sensors, Sens. Actuators, B 22 (1994) 27-35.

[13] S. Matsushima, Y. Teraoka, N. Miura, N. Yamazoe, Electronic interaction between metal additives and tin dioxide in tin dioxide-based gas sensors, Jpn. J. Appl. Phys. 27 (1988) 1798-1802.

[14] S. C. Tsang, C. D. A. Bulpitt, P. C. H. Mitchell, A. J. Ramirez-Cuesta, Some new insights into the sensing mechanism of palladium promoted tin (IV) oxide sensor, J. Phys. Chem. B 105 (2001) 5737-5742.